ELECTROCHROMIC WINDOW WITH LITHIUM CONDUCTIVE POLYMER ELECTROLYTE

Paul Baudry[1], Michel Andre' Aegerter[1], Daniel Deroo[2], Bruno Valla[2]

[1]Instituto de Fisica e Quimica de São Carlos,
University of São Paulo
C.P. 369, 13560 São Carlos BRAZIL

[2]Laboratoire d'Ionique et d' Electrochimie du Solide
ENSEEG BP 75 Domaine Universitaire
38402 Saint Martin d' Heres. FRANCE

ABSTRACT

An electrochromic window was built using WO_3 as the electrochromic material and V_2O_5 as the counter-electrode. Both were deposited onto ITO coated glass panes by vacuum evaporation and were amorphous to X-ray diffraction. The electrolyte was a lithium conducting polymer constituted by a Poly (ethylene oxide) - lithium salt complex. The electrochemical characterization of electrodes was realized by cyclic voltammetry, coulometric titration, and impedance spectroscopy, which allowed the determination of the chemical diffusion coefficients of lithium into WO_3 and V_2O_5. Potentiostatic cycling of the complete transmissive cell yields a transmission variation from 41% to 13% at 633 nm with a response time of 10 seconds at room temperature.

1. INTRODUCTION

Over the last two decades, much work has been dedicated to the study of electrochromism for its possible application in electro-optical devices (1,2). However, some major problems such as slow switching time or corrosion layers have been encountered. Nevertheless, the realization of energy efficient windows emerged a few years ago as a new, interesting application in that field (3,4). In this latter kind of device, a response time of approximatively

one minute, easily attainable, is sufficient, and the memory effect provided by the electrochemical reaction is of great interest.

Many insertion materials, for instance metal transition oxides, exhibit electrochromic properties when deposited in thin films. Their optical properties are modified by electrochemical insertion of alkali cations or protons. The corresponding reaction can be written as:

$$yA^+ + ye^- + MO_x \longrightarrow A_yMO_x$$

Tungsten trioxide has been the most investigated electrochromic material (5,6) and without any doubt is one of the most promising with respect to its electrochromic properties. Both proton and lithium insertion are possible. Although the chemical diffusion coefficient of H^+ in WO_3 is higher than that of Li^+ (7), it seems easier to realize a complete transmissive electrochromic device with lithium conductors than with protonic ones, as hydrogen gassing and layer corrosion in acid media are major drawbacks in the protonic system.

Polymer electrolytes have been widely studied during the last ten years for making high energy secondary solid-state batteries (8,9). Their use in electrochromic devices is suitable since they can be fabricated in thin elastomeric films, and do not present problems of leakage encountered with liquid electrolytes. Poly(ethylene oxide) (PEO) complexes exhibit conductivities higher than 10^{-5} $\Omega^{-1}cm^{-1}$ with both lithium and proton conduction (10,11) giving rise to fast switching times.

Whereas, the electrochromic material and a solid electrolyte are available, a suitable transparent counter-electrode is still to be found. Two different types of counter-electrode can be considered. It may be transparent at both oxidized and reduced states, but a "rocking chair" counter-electrode, colouring at the same time as the electrochromic electrode may also be envisaged. In this latter case, the counter-electrode will color anodically, if WO3 is used as electrochromic material. For example, IrO_2 has been successfully used with protonic conduction (12).

In this work, a Li_xWO_3/lithium conducting polymer electrolyte/ $Li_xV_2O_5$ electrochromic window is investigated. V_2O_5 has been selected as a counter-electrode because it is a good lithium insertion material and is fairly transparent in thin films (12). The reversible insertion reaction can be written as follows:

$$V_2O_5 + yLi^+ + ye^- \longrightarrow Li_yV_2O_5$$

Individual layers have been characterized by SIMS, cyclic voltammetry and AC impedance. Potentiostatic cycling, coupled with transmittance measurements was performed at room temperature on the complete device in order to evaluate the performance of the cell.

2. EXPERIMENTAL

2.1 Layers preparation

Both WO_3 and V_2O_5 layers were deposited from the corresponding oxide powder by vacuum evaporation onto 0.4 μm thick indium tin oxide (ITO) coated glasses. These films were amorphous to X-ray diffraction. Their thickness, measured by a Talystep within an accuracy of ± 10 nm, was 220 nm for V_2O_5 and varied from 200 to 300 nm for WO_3. The films were electrochemically characterized as deposited without any heat-treatment.

The polymer electrolyte was a poly(ethylene oxide)-LiX complex ($X=ClO_4$, $N(SO_2CF_3)_2$). It was prepared by dissolving PEO powder (m.w.=$5x10^6$) and the lithium salt in acetonitrile, with a O:Li atomic ratio of 8:1, giving rise to the highest conductivity in these systems (9,10). This viscous complex was doctor-bladed on a polytetrafluoroethylene substrate. Then, the solvent was evaporated at 70°C for 24 hours. The polymer films were kept in a dry box (< 1 ppm H_2O) in order to eliminate any residual solvent or moisture. Elastomeric thin films (50 to 200 μm) were thus obtained.

2.2 Secondary Ion Mass Spectroscopy (SIMS)

Profiles of lithium concentration within the electrode layers were measured by SIMS at different insertion rates. For this purpose, a previous electrochemical insertion was made in an acetonitrile-0.1 M $LiC10_4$ electrolyte. The counter-electrode was a platinum foil and the reference was constituted by a silver wire immersed in an acetonitrile 00.01M $AgNO_3$ solution. The reference compartment was separated from the main cell by a fritted glass tube. The potentiostatic mode was preferred to the galvanostatic one to realize the reduction in order to avoid any side reaction. The potential applied was -1.5V/Ag. The SIMS experiments were performed with a 5.5 keV O_2^+ beam and an intensity of 30 nA.

2.3 Electrochemical experiments

Cyclic voltammetry, coulometric titration and AC impedance measurements were performed with PEO-$LiClO_4$ polymer electrolyte. The cells were hot-pressed at 80°C in the dry box and sealed with a low vapour pressure paste (Varian Torr-seal). A 1.6 cm diameter lithium disk covered by stainless steel was used as counter and reference electrode in the cyclic voltammetry and coulometric titration cells. The use of the same electrode as counter and reference electrodes was justified by the low polarisability of the lithium, especially at high temperature and with low currents flowing through the cell. The AC impedance was realized with a two-electrode configuration as shown in Fig. 1. Working and counter electrodes were constituted by the same material with the same insertion rate. A lithium reference was placed beside the working electrode in order to control the potential and to be able to reduce both counter and working electrodes at the same potential before executing the impedance measurements. After reaching equilibrium, i.e. the stabilization of potential, a small alternating voltage was applied between the two electrodes. The impedance was measured with a frequency response analyser (Solartron 1250) coupled to an Apple IIC calculator in the frequency range $6x10^{4}$-10^{-3}Hz at several temperatures. In this configuration, the measured impedance is the sum of the working electrode, counter electrode and electrolyte impedances.

For the cycling tests, it is necessary to reduce either the WO_3 or V_2O_5 electrode before assembling the cell in order to obtain a lithium reservoir. Although this reduction can be made chemically, for example by reaction with n-butyllithium in a non polar solvent like cyclohexane,
the electrochemical way was preferred. It provides a more homogeneous and faster colouration, and the insertion rate can be controlled. In this complete window, the electrolyte was a PEO-$LiN(SO_2CF_3)_2$ complex which is more conductive and transparent than the PEO-$LiClO_4$ electrolyte at room temperature, due to a lower glass transition temperature (10). This transmissive device was also hot-pressed and sealed in the dry box in order to avoid any moisture contamination. Its optical transmission was measured at 633 nm (He-Ne laser) simultaneously with the current flowing through the cell.

3. RESULTS AND DISCUSSION

The WO_3 and V_2O_5 layers have been analyzed by SIMS technique at different insertion rates. The profiles of lithium concentration in these layers are represented in Fig. 2 and 3. The concentration gradient of lithium in

WO_3 is low till the WO_3/TTO interface, but is very high in ITO. In V_2O_5, it is low also till the V_2O_5/ITO interface for high lithium concentration. This means that the lithium diffusion in ITO is very slow as it is expected to be fast in WO_3 and V_2O_5. In both cases, the lithium concentration is nearly proportional to the charge passed through the cell. However, the values of the lithium concentration obtained for both materials cannot be compared quantitatively because their erosion rates by the incident beam are different.

Figures 4 and 5 show the cyclic voltammetries obtained at 80°C with PEO-$LiClO_4$ electrolyte for WO_3 and V_2O_5 electrodes, respectively. The shape of the WO_3 voltammogram is the same as that obtained with a liquid electrolyte. Even at low sweep rate, no insertion peak has been observed. Armand (13) reported that this peak is located at 1.5 V/Li. This potential value is outside the scanned range because the stability threshold of ITO is approximately 1.7 V/Li. It is also well known that crystalline V_2O_5 exhibits in cyclic voltammetry three well-defined peaks corresponding to three different phases (14). In the V_2O_5 voltammogram of Fig. 5, we only observe one peak at 2V/Li and a broad shoulder at 3V/Li. This behaviour is therefore characteristic of an amorphous electrode.

The thermodynamic curves of Fig. 6 and 7 have been obtained by coulometric titration, i.e. a succession of galvanostatic pulses and potential equilibration. We can observe that the potential decreases monotonically when the lithium insertion rate increases, which confirms the amorphous electrode behaviour. With a multiphase electrode material, one would observe plateaus in the thermodynamic curve. The available insertion rate above 2 V/Li obtained by calculating the number of lithium ions inserted by metal atom, is 0.8 for WO_3 and 0.9 for V_2O_5. These values are in good agreement with those reported by Mohapatra et al. (15) for amorphous WO_3 in liquid electrolyte and by Nabavi et al. (16) for amorphous bulk V_2O_5 electrode.

The ac response of an electrochemical system with either charge transfer or diffusion-limited kinetics has been analyzed by Randles (17) with the equivalent circuit shown in Fig. 8, and applied by Ho et al. (18) to the case of lithium insertion in amorphous WO_3 with a liquid electrolyte. In this figure, R_E is the ohmic resistance of the electrolyte, θ is the charge transfer resistance, C_{DL} is the double layer capacitance of the electrode/electrolyte interface, and Z_D is a complex impedance arising from the diffusion of lithium ions.

The charge transfer resistance θ is related to the exchange current density i_o through a linearization of the Butler-Volmer equation for small overpotentials (19):

$$\theta = \frac{R\,T}{z\,F\,i_o}S \qquad [1]$$

where R is the gas constant, T is the temperature, z is the charge of the inserted cation, F is the Faraday, and S is the surface area. The expression of Z_D can be obtained by the resolution of the Fick equation with suitable initial and boundary conditions:

$$Z_D = \frac{L\,V_M}{z\,f\,S\,\tilde{D}}(dE/dy)_{y_o}\frac{1}{u}\coth u \qquad [2]$$

$$\text{with } u = L(jw/\tilde{D})^{1/2}$$

and where $j = \sqrt{-1}$, L is the film thickness, V_M is the molar volume, $\tilde{D}$ is the chemical diffusion coefficient, $(dE/dy)_{y_o}$ is the slope of the coulometric titration curve at the insertion rate y_o, w is the radial frequency, and u is a nondimensional number characterizing the mode of diffusion.

The WO_3 and V_2O_5 impedance data shown in Fig. 9 and 10 have been plotted in the Nyquist plane at different temperatures. The semicircle observed at high frequencies which is related to the charge transfer process, is well separated from the low frequency part of the diagram corresponding to the lithium diffusion into the electrode material. Therefore, the charge transfer resistance, and consequently, the exchange current density through equation [1], have been calculated at different temperatures and are shown in Fig. 11. At low temperature, i_o is small and the charge transfer process may be the limiting step for fast switching times. This emphasizes the problem of a solid/solid interface and the importance of a good electrolyte/electrode contact.

Ho et al. (18) have considered two extreme cases for the determination of the chemical diffusion coefficient:

1. When $\tilde{D}/wL^2 \ll 1$, the semi-infinite diffusion conditions are fulfilled, giving rise to the Warburg impedance:

$$Z_D = \frac{V_M\,(dE/dy)}{\sqrt{2}\,z\,F\,\tilde{D}^{1/2}\,S}\,w^{-1/2}(1-j) \qquad [3]$$

The current is $\Pi/4$ out of phase with the voltage, and $\tilde{D}$ can be calculated if S and dE/dy are known.

2. When $\tilde{D}/wL^2 >> 1$, the homogeneous diffusion regime is obtained. Under this condition, the real part of the impedance Re(Z) is independent of the frequency:

$$Re(Z) = \frac{V_M L}{z F S 3\tilde{D}} \qquad [4]$$

Thus, the phase difference between the current and the voltage is equal to $\Pi/2$, and $\tilde{D}$ can be calculated without the knowledge of S and (dE/dy) by the relation:

$$\tilde{D} = \frac{L^2 w}{3 Re(Z)} \; Im(Z) \qquad [5]$$

where Im(Z) is the imaginary part of the impedance. It must be pointed out that only the diffusion part must be taken into account for Re(Z).

These two limiting cases are theoretically very convenient for the determination of $\tilde{D}$. However, they are not easy to use with the impedance diagrams that we obtained. On one hand, the Warburg portion is small and probably hidden in the charge transfer zone. On the other hand, the accuracy in the determination of Re(Z) in the low frequency part is very poor. Actually, the impedance is not purely capacitive, and Re(Z) is slightly dependent on the frequency. This can be attributed to a dispersion phenomenon due to a weak lithium diffusion from WO_3 into ITO or a contact loss at the electrolyte/electrode interface, giving rise to a non planar electrode. Therefore, we have considered the intermediate case where $\tilde{D}/wL^2$ is close to 1. The equation [2] enables a direct relation between the phase and $\tilde{D}/wL^2$ as shown in Fig. 12. In the range of intermediate frequencies, the phase variation is large, increasing the accuracy. Thus, $\tilde{D}$ has been calculated for a phase equal to $\Pi/3$. The temperature dependence of the lithium chemical diffusion coefficient in WO_3 and V_2O_5 obtained by this method is shown in Fig. 13. This yields values of 2.5×10^{-11} cm^2/s for WO_3 at 2.4V/Li and 2.5×10^{-12} cm^2/s for V_2O_5 at 3V/Li at 25°C. These values have to be compared with those determined also by impedance spectroscopy but with a liquid electrolyte. Ho et al. (18) reported a $\tilde{D}$ value of $1.5\ 10^{-11}$ cm^2/s at the same voltage in propylene carbonate-$LiAsF_6$ solution for WO_3 and Zachau et al. (20) obtained $\tilde{D} = 6.3\ 10^{-12}$ cm^2/s with crystallized V_2O_5 in propylene carbonate-$LiClO_4$ at 2.8V/Li. The concordance is good as this method does not take into account the surface area. Therefore, the main modification introduced by the presence of a solid/solid interface involves only the charge transfer process whereas the diffusion kinetics is the same as with a liquid electrolyte.

The $10,000^{th}$ cycle of a potentiostatic test carried out with a WO_3/PEO-$LiN(SO_2CF_3)_2/V_2O_5$ electrochromic window at room temperature is shown in Fig. 14. The optical transmission at 633 nm varies from 41% in the bleached state to 13% in the coloured state with a time response of 10 s. The major drawback remains the low optical transmission value in the bleached state.

4. CONCLUSION

The use of a solid polymer electrolyte in an electrochromic device allowed us to study the lithium insertion reaction into WO_3 and V_2O_5 under anhydrous conditions. The absence of humidity confers to the system a memory effect of several months. By impedance spectroscopy, the charge transfer and diffusion processes have been separated. The lithium chemical diffusion coefficient has been determined by a method which does not involve the value of the electrode surface area. These $\tilde{D}$ values were found similar to those obtained with liquid electrolytes. The main difference introduced by the presence of a solid/solid interface is the low exchange current density at room temperature. Therefore, the importance of a good electrolyte/electrode contact has been underlined. This could be probably improved by using a polymer electrolyte of lower molecular weight. The feasibility of an all solid state WO_3/V_2O_5 transmissive device has been demonstrated. The main drawback remains the residual colouration in the bleached state. In order to improve the transmission characteristics and to obtain a reversible transparent counter-electrode exhibiting fast insertion kinetics, we have recently prepared in our laboratory mixed cerium titanium oxides layers by the dip-coating process with encouraging results (21). Multicomponent oxide layers can be obtained by this technique which can substitute other physical methods of deposition for the search of an ideal counter-electrode.

ACKNOWLEDGMENTS

The authors acknowledge the technical and financial support of Saint Gobain Recherche in France and the financial help of CNPq in Brazil.

5. REFERENCES

1. S. K. Deb, Applied Optics, suppl. 3. 192 (1969).
2. W. C. Dautremont-Smith, Displays 3, 3 (1982).
3. C. M. Lampert, Solar Energy Materials 11, 1 (1984).
4. R. C. Rauh, S. F. Cogan, and M. A. Parker, Proc. SPIE 502, 38 (1984.
5. M. Greene, W. C. Smith, and J. A. Weiner, Thin Solid Films, 38, 89 (1976).
6. S. K. Mohapatra, J. of Electrochem. Soc., 125, 284 (1978).
7. J. P. Randin and R. Veinnet, J. Electrochem. Soc. 129 (10) 2349 (1982).
8. M. B. Armand, J. M. Chabagno, and M. Duclot, Fast Ion Transport in Solids - T. Vashita Ed. North Holland - New York 131 (1979).
9. M. B. Armand, Solid State Ionics 9-10, 745 (1983).
10. M. B. Armand, W. Gorecki, A. Andreani, 11th International Conference on Polymer Electrolytes, Siena Italia, June 14-16, 1989.
11. P. Donoso, W. Gorecki, C. Berthier F. Defendini, and M. Armand, Solid State Ionics 28-30 (1988).
12. R. D. Rauh and S. F. Cogan, Solid State Ionics 28-30, 1707 (1988).
13. M. B. Armand, Ph.D. Thesis, Grenoble (1978).
14. P. G. Dickens and G. J. Reynolds, Solid State Ionics 5, 331 15 (1981).
15. S. K. Mohapatra, S. Wagner, J. or Electrochem. Soc. 125, 1603 (1978).
16. M. Nabavi, C. Sanchez, F. Tautelle, and J. Livage, Solid State Ionics, 28-30, 1183 (1988).
17. J.E.B. Randles, Discuss. Faraday Soc. 1, 11 (1947).
18. C. Ho, I. D. Raistrick, R. A. Huggins, J. Electrochem. Soc. 127, 2 343 (1980).
19. A. J. Bard and L. R. Faulkner, Electrochimie, Masson Ed., p. 116 (1983).
20. B. Zachau-Christiansen, K. West, and T. Jacobsen, Solid State Ionics 9-10, 399 (1983).
21. P. Baudry, A. C. Rodrigues, M. A. Aegerter, and L. O. Bulhoes, Proc. Fifth Int. Workshop on Glasses and Ceramics from Gels, Rio de Janeiro, August 6-10, 1989.

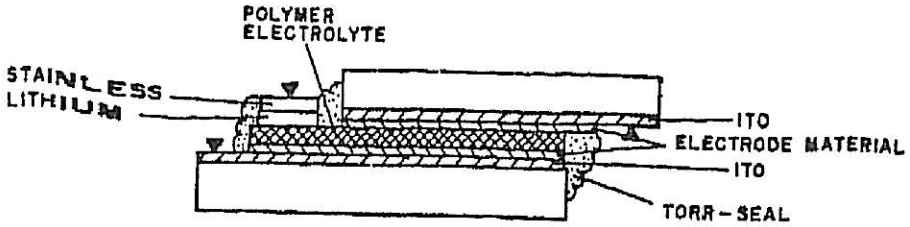

Figure 1. Experimental set-up for impedance measurments with PEO-$LiClO_4$ polymer electrolyte

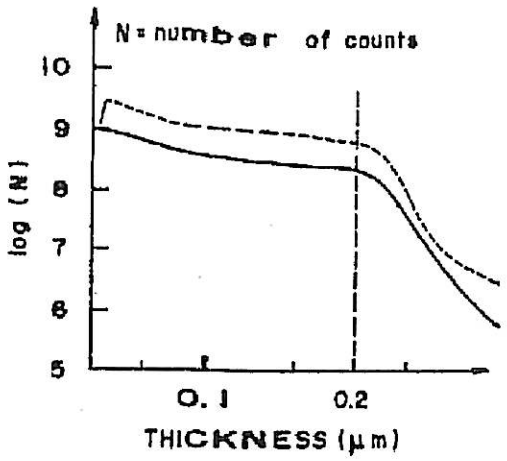

Figure 2

Profile of lithium concentration in WO_3 by SIMS —— 12,2 mC/cm^2 ——— 22 mC/cm^2

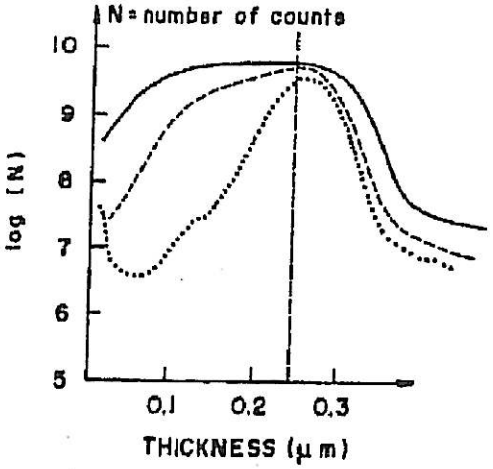

Figure 3

Profile of lithium concentration in V_2O_5 by SIMS —— 19,4 mC/cm^2 —— 10,6 mC/cm^2, ... 6,2 mC/cm^2

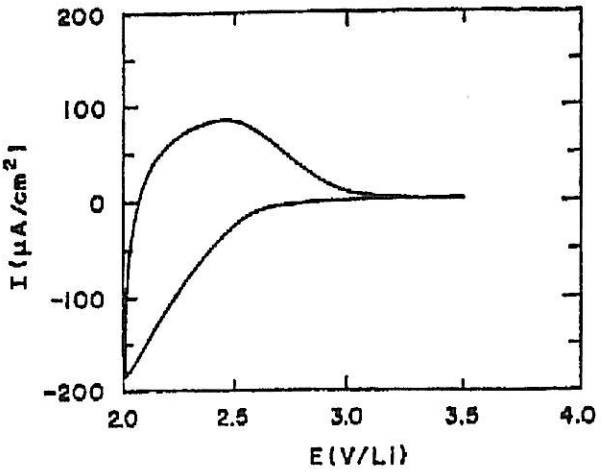

Figure 4

Cyclic Voltammetry of a 300 nm thick WO_3 electrode

PEO-$LiClO_4$ electrolyte, T= 80°C

sweep rate: 300 mV/s

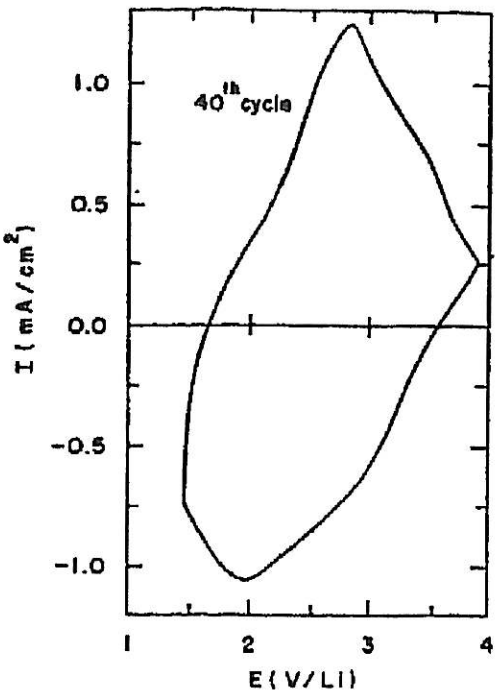

Figure 5

Cyclic Voltammetry of a 220 nm thick V_2O_5 electrode

PEO-$LiClO_4$ electrolyte, T= 80°C,

sweep rate: 1000mV/s

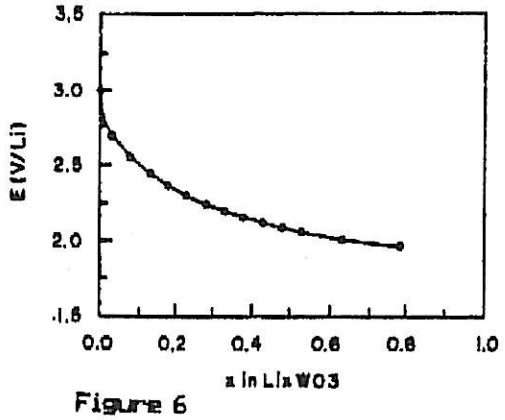

Figure 6

Coulometric titration curve for WO_3 electrode with PEO-$LiClO_4$ electrolyte, T= 80°C

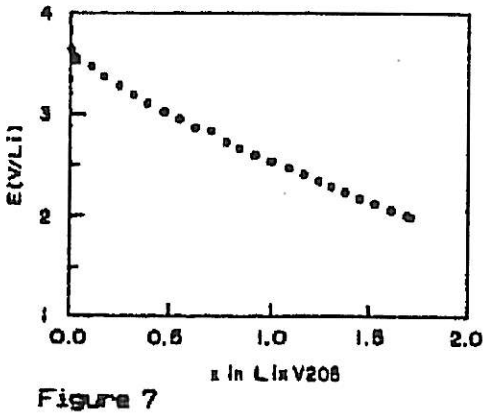

Figure 7

Coulometric titration curve for V_2O_5 electrode with PEO-$LiClO_4$ electrolyte, T= 80°C

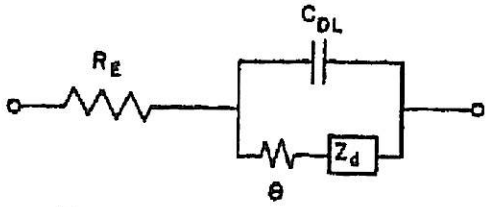

Figure 8

Randles equivalent circuit

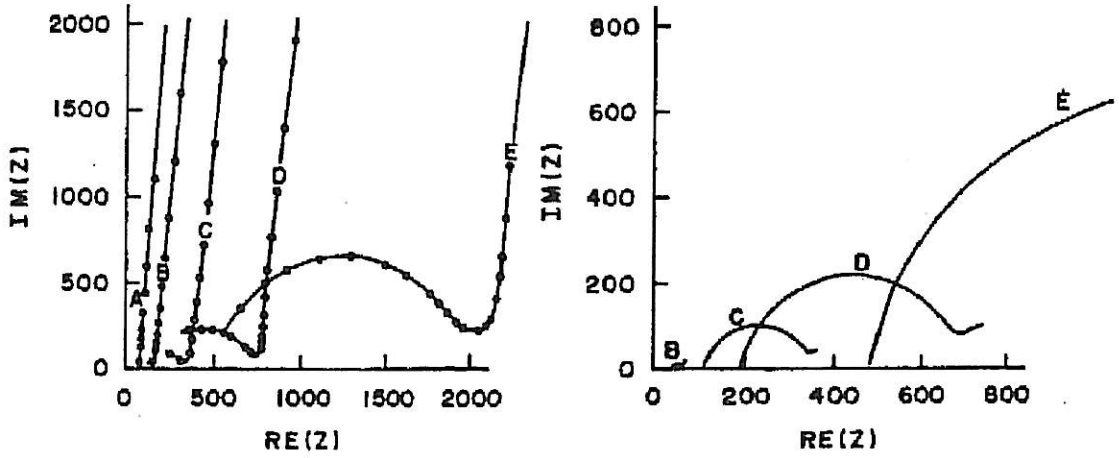

a) b)

Figure 9

Complex impedance data for 200 nm thick WO_3 electrode (2.4V/Li) with PEO-$LiClO_4$ electrolyte

a. low frequencies plot b. high frequencies plot

A: 81°C B: 65°C C: 55°C D: 45°C E: 36°C

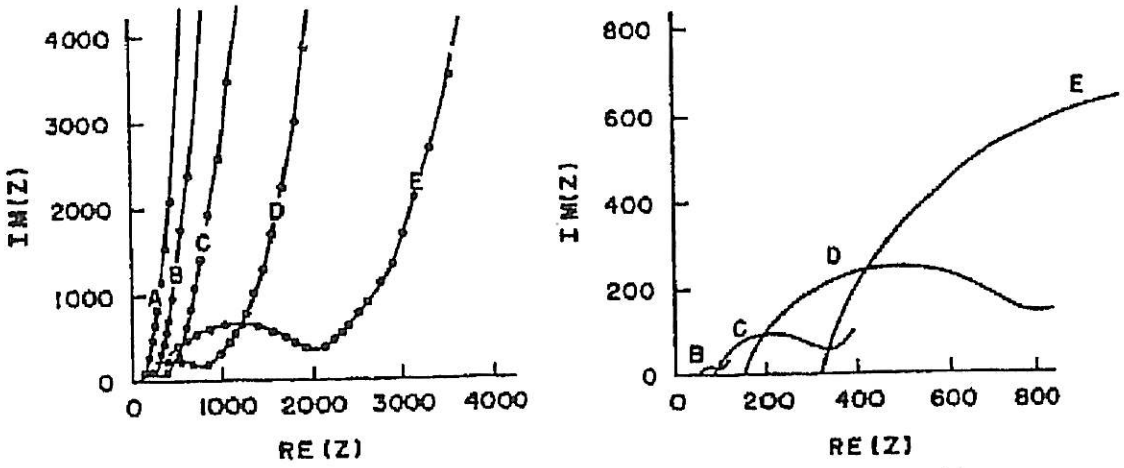

Figure 10

Complex impedance data for 220 nm thick V_2O_5 electrode (3V/Li) with PEO-$LiClO_4$ electrolyte

a. low frequencies plot b. high frequencies plot

A: 87°C B: 74°C C: 66°C D: 55°C E:45°C

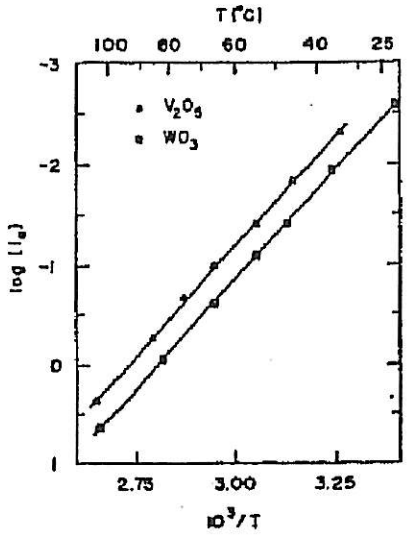

Figure 11

Temperature dependence of i_0 (mA/cm^2) with PEO-$LiClO_4$ electrolyte for WO_3 and V_2O_5 electrodes

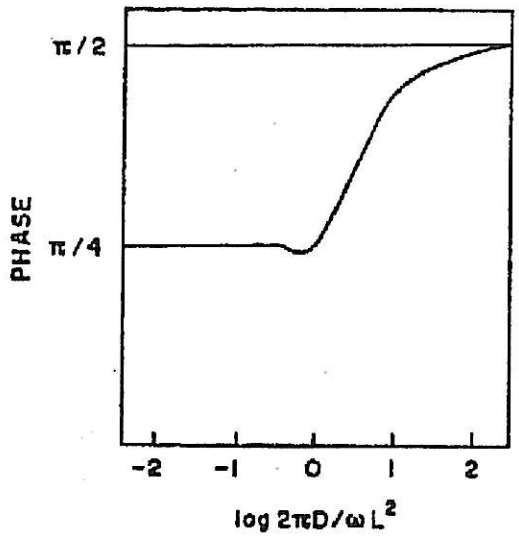

Figure 12

relation between the impedance phase and $\tilde{D}$ calculated through equation (2)

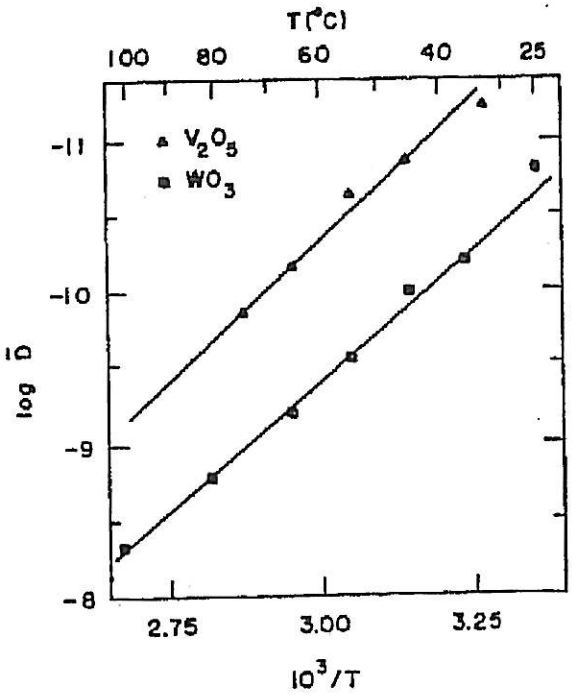

Figure 13

Temperature dependence of

$\tilde{D}$ (cm^2/s) for WO_3 and V_2O_5

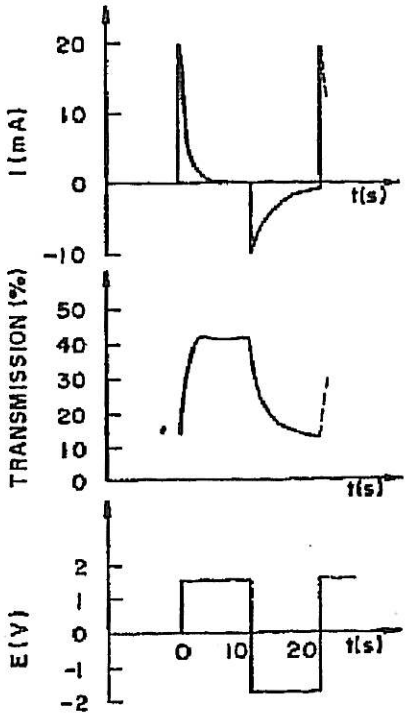

Figure 14

10.000th cycle of a potentiostatic test on an electrochromic window WO_3/ PEO-LiN$(SO_2CF_3)_2$ / V_2O_5 transmission at λ= 633 nm